Bull Mater Sci (2020)43:206
https://doi.org/10.1007/s12034-020-02171-x

Initiatively embedding silver colloids in glass used in silver paste to improve metallization ohmic contact on silicon wafers

GUOQING LI, XINJIE SUN, HUA TONG*, JIEFENG ZHANG, HUI LI, YUNXIA YANG, HONGBO LI and XIAO YUAN

Key Laboratory for Ultrafine Materials of Ministry of Education, School of Materials Science and Engineering, East China University of Science and Technology, Shanghai 200237, People's Republic of China
*Author for correspondence (tonghua@ecust.edu.cn)

MS received 19 December 2019; accepted 26 February 2020

Abstract. One of the decisive factors in realizing ohmic contact of silver (Ag) paste metallization on silicon (Si) wafers is the presence of Ag colloids in the glass phase at the Ag/Si interface. The Ag colloids are formed during the reaction between glass frit and Ag powder in the sintering process of Ag paste; thus, it is difficult to control the quantity of Ag colloids formed. In this study, we attempted to prepare a glass embedded with a large number of Ag colloids first to further improve the quality of ohmic contact of Ag paste metallization. In the $PbO–TeO_2–SiO_2$ glass system, a route was found for increasing the solubility of Ag in the glass melt by precipitating the $Ce_{1.88}Pb_{2.12}O_{6.53}$ crystal, which enabled a molar amount of recrystallized Ag colloids reach a high level of about 1/10 of oxides in the glass. As a result, the resistivity of the Ag/Si contact can be decreased substantially. The formation mechanism of Ag colloids in glass is revealed by various characterization and analysis methods, such as X-ray diffraction, electron energy loss spectroscopy, X-ray photoelectron spectroscopy, UV–visible and so on. Furthermore, it was also found that too high content of Ag in the glass melt would destroy the pyramid texture surface structure of Si wafers, which is not conducive to obtain high-quality Ag/Si ohmic contact. For this concern, optimal content of Ag colloids formed in glass is discussed.

Keywords. Silver colloids; silver paste; silicon wafers; metallization; ohmic contact.

1. Introduction

The urgent need to continuously improve the efficiency of commercial crystalline silicon (c-Si) solar cells poses great challenges to silver (Ag) paste metallization technology, because the electrical performance of metallized Ag/Si contact has an increasingly important impact on the efficiency of the cells [1]. Ag paste metallization on Si wafers produces a special Ag/glass/Si interface structure, which enables the carrier transport by the tunnelling mechanism [2]. From the point of view of classical quantum theory, electrons can only tunnel through several nanometres of insulating media. In fact, however, the thickness of the glass phase in the Ag/Si interface can reach tens to hundreds of nanometres. This is because a large number of Ag colloids with sizes ranging from several nanometres to tens of nanometres are embedded in the glass phase. The mechanism of carrier transport through this contact interface has received extensive attention, and a convincing explanation called percolation mechanism has been proposed recently [3].

During Ag paste metallization on Si wafers, the formation of Ag colloids in the glass phase involves very complex physical and chemical reactions. It was often observed that Ag colloids precipitated at the interface between the glass phase and sintered Ag grains, which were thought to be the product of reduction of Ag ions on the surface of Ag grains by metallic lead elements in glass [4]. In contrast, the Ag colloids formed in glass were considered as the result of recrystallization of Ag that dissolved during the heating process [5]. In addition, larger Ag microcrystals formed by reducing Ag ions with Si were sometimes observed pinning into the Si surface [6].

Because increasing the quantity of Ag colloids in the glass phase can effectively reduce the Ag/Si contact resistance, a few researchers tried to change the process parameters of sintering of Ag paste [7], such as increasing peak temperature or prolonging sintering time, to dissolve more Ag in the glass phase [8]. However, this would sometimes lead to serious erosion to Si emitter surface, resulting in large leakage or p–n junction damage. Ways exist to facilitate Ag precipitation by introducing an oxygen

Electronic supplementary material: The online version of this article (https://doi.org/10.1007/s12034-020-02171-x) contains supplementary material, which is available to authorized users.

Published online: 13 August 2020

atmosphere during the sintering of Ag paste, however this method is not suitable for commercial production lines. Because of short time taken for sintering of Ag paste by cell production lines [9], it is also difficult to increase substantially the amount of Ag colloids formed in the glass phase by only adjusting glass composition to enhance the reactivity with Ag. In the current study, we thus propose to embed Ag colloids in glass beforehand. Taking the PbO–TeO_2–SiO_2 glass system for exemplification, we demonstrate that a large amount of Ag colloids can grow in glass with assistance by cerium oxide, and the application performance of such treated glass in Ag paste metallization is investigated in depth.

2. Experimental

2.1 *Materials*

All materials were not purified further before use. Glasses were prepared by melt-quenching in water. Firstly, the raw materials (see the description in table 1) were thoroughly mixed and then transferred into an alumina crucible to heat in an electric furnace at 1000°C for 1 h. In this process, Ag particles with a diameter of 50 nm were used. The glass melt was poured into deionized water at room temperature, and the solidified glass bulk was ground into small particles with a D_{50} size of about 2.5 μm by using the high-energy ball mill. Ag paste was prepared by using a three-roll machine, which was composed of 80 wt% Ag powder (with spherical morphology and average diameter size of 1.2 μm), 2.5 wt% glass frit and 17.5 wt% organic carrier.

2.2 *Printing and sintering of Ag paste samples*

2.2a *Transmission-line modelling (TLM) samples*: On monocrystalline Si wafers, Ag paste was printed into electrode lines with a width of 0.5 mm, height of 18–20 μm, length of 20 mm and spacing of 1 mm. The printed wafers were baked at 250°C for 3 min, and then fired in an open infrared furnace by a three-step heating process. The temperature control process is as follows: temperature raised from room temperature to 550°C in 60 s, then to 700°C in 9 s and maintained at 700°C for 9 s.

2.2b *Solar cell samples*: The Ag-free glass (no. 5) and Ag-containing glass (no. 7) were selected respectively as the inorganic component of Ag paste, which was used in the front-side metallization of passivated emitter and rear cells. Supplementary figure S1 presents the digital images of a typical c-Si solar cell prepared in our study. The p-type monocrystalline Si wafers (15.6 × 15.6 cm^2) were employed. The front surface of the wafers was textured, diffused with phosphorus to form n^+ emitters with 80 Ω sq^{-1} sheet resistance, and deposited with an 80 nm thickness Si_3N_x passivation layer. The back surface of Si wafer was deposited with a passivation layer consisting of around 10 nm thickness Al_2O_3 (bottom) and around 130 nm thickness Si_3N_x (top). In the fabrication of two kinds of solar cells, two different front Ag pastes (containing no. 5 glass and no. 7 glass, respectively) but the same commercial Al rear paste and Ag rear paste were used to prepare front an Ag gridline electrode, alloyed Al back surface field and Ag back electrode by the screen printing method. On the front side of Si wafer, the Ag paste was printed into five busbars and 96 fine fingers. The printed line width was about 0.7 mm for busbars and about 33 μm for fine fingers. The printed Si wafers were fired in a nine-temperature-region belt furnace (Despatch, USA) at a set peak temperature of 910°C and belt speed of 230 in. min^{-1}.

2.3 *Characterization and measurements*

The Ag/Si contact resistance was measured by the TLM method. Field emission-scanning electron microscopy (FE-SEM, Hitachi S-4800) was used to study the micromorphology of the samples. The optical absorption of glass samples was studied by using an ultraviolet–visible spectrophotometer (UV–visible). X-ray photoelectron

Table 1. Description of raw materials used in glass melting.

	Oxides used as glass composition (mol%)								
No.	PbO	TeO_2	Bi_2O_3	SiO_2	Li_2O	ZnO	CeO_2	Ag	Ratio of Ag to oxides
1	25	30	7.5	12	15	5	0	0	0:94.5
2	25	30	7.5	12	15	5	0	1	1:94.5
3	25	30	7.5	12	15	5	0	5	5:94.5
4	25	30	7.5	12	15	5	0	10	10:94.5
5	25	30	7.5	12	15	5	5	0	0:99.5
6	25	30	7.5	12	15	5	5	1	1:99.5
7	25	30	7.5	12	15	5	5	5	5:99.5
8	25	30	7.5	12	15	5	5	10	10:99.5

spectroscopy (XPS) and electron energy loss spectroscopy (EELS) were used to identify the valence states of elements in the glass phase. The composition of the glass phase was characterized by X-ray diffraction (XRD). The doping concentration on the surface of the metallized Si emitter was measured by the electrochemical capacitance–voltage (ECV) method. The electrical parameters of solar cells were measured on a photovoltaic *I–V* test system under AM1.5 spectrum at the temperature of 25°C.

3. Results and discussion

3.1 *Formation of Ag colloids in glass*

In the preparation of glasses, the mixture of raw materials, including oxides and Ag powder in a specific molar ratio (table 1) was melt at 1000°C for 1 h, and then cooled rapidly to room temperature by quenching in water. This manipulation was aimed to dissolve a large amount of Ag atoms in glass melt at high temperature and crystallize them into colloids during the cooling process. However, little Ag was dissolved in the cerium (Ce)-free glass. The millimetre-sized metallic particles can be observed in the melt-quenching products (supplementary figure S2a), for which the molar ratio of Ag to oxides was 1:94.5 in the raw material. By XRD characterization (figure 1a), it was confirmed that the products contained some Ag crystals, which were separated from the glass phase, implying a quite low solubility of Ag in the glass melt.

We found that the solubility of Ag in glass melt can be improved greatly by adding a small amount of cerium oxide to the raw material. In the current study, cerium oxide accounted for 5/99.5 (molar ratio) of the oxides. Ag crystals did not emerge in the melt-quenching products when the molar ratio of Ag to oxides ranged from 1:99.5 to 10:99.5, whereas the colour of glass bulks changed from yellow to dark red (supplementary figure S2b). The XRD pattern (figure 1b) of glass exhibited a broadening peak of amorphous substance and characteristic diffraction peaks of the $Ce_{1.88}Pb_{2.12}O_{6.53}$ crystal (PDF no. 89-3722). In contrast, when Ag powder was not added in the preparation of glasses, only a broadening peak of amorphous substance existed in the XRD pattern of the products (figure 1c). The uniform distribution of Ce element in the Ag-free glass was observed by elemental imaging of energy dispersive spectroscopy (EDS) in transmission electron microscopy (figure 2a and b). Figure 2c shows the EELS of Ce element in glass. According to the M5/M4 peaks at 885 and 903 eV, the valence state of Ce element was determined to be positive tetravalent [10]. However, Ce element can hardly be detected in the glass prepared with the addition of Ag. This indicates that the dissolution of Ag in the glass phase was closely related to the precipitation of the $Ce_{1.88}Pb_{2.12}O_{6.53}$ crystal.

Ag can be dissolved in the glass phase in two ways. One is the diffusion of zero-valent Ag^0 atoms into the glass network, but the solubility is relatively small. Another is that Ag is oxidized, and then Ag^+ and O^{2-} ions are absorbed into the glass network together. In this way, Ag can have a high solubility in the glass phase due to the increase of free-O^{2-} ion content [11]. However, Ag^+ ions in the glass network usually do not crystallize into colloids, but play the role of a network modifier [12]. XPS analysis (figure 3a) shows that the major part of Ag element in the currently prepared glasses was zero-valent according to the $3d_{5/2}$ peak of 368.2 eV and the $3d_{3/2}$ peak of 374.1 eV, and the minor part of Ag element was positive one-valent based on the $3d_{5/2}$ peak of 367.8 eV and $3d_{3/2}$ peak of 373.7 eV [13].

Based on XPS analysis, lead element in the glass phase had both divalent and tetravalent states (figure 3b), and nearly 70% of lead element was tetravalent in the $Ce_{1.88}Pb_{2.12}O_{6.53}$ crystal. Therefore, it is inferred that the dissolution of Ag in the glass phase underwent the following processes:

$$Ag^0 + O_2 \rightarrow Ag^+ + O^{2-} \quad (1)$$

$$Ag^+ + Pb^{2+} \rightarrow Ag^0 + Pb^{4+} \quad (2)$$

$$Pb^{4+} + Pb^{2+} + Ce^{4+} + O^{2-} \rightarrow Ce_{1.88}Pb_{2.12}O_{6.53} \quad (3)$$

Accordingly, tetravalent Ce^{4+} ions were used as nucleating agents. With the precipitation of the $Ce_{1.88}Pb_{2.12}O_{6.53}$ crystal, Ce^{4+} and Pb^{4+} ions were removed from the glass phase, and the reduction of Ag^+ ions becomes easier, thus the solubility of Ag in the glass phase was increased.

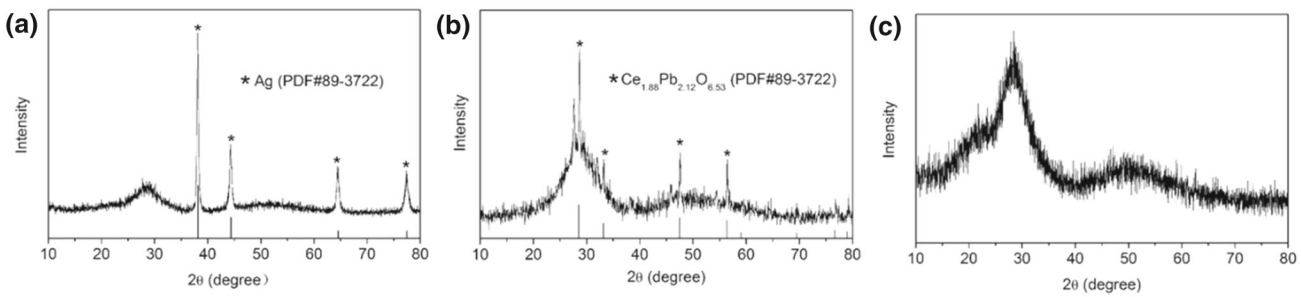

Figure 1. XRD patterns of products from glass preparation using different raw materials: (**a**) Ag powder and oxides not including CeO_2; (**b**) Ag powder and oxides including CeO_2 and (**c**) oxides including CeO_2.

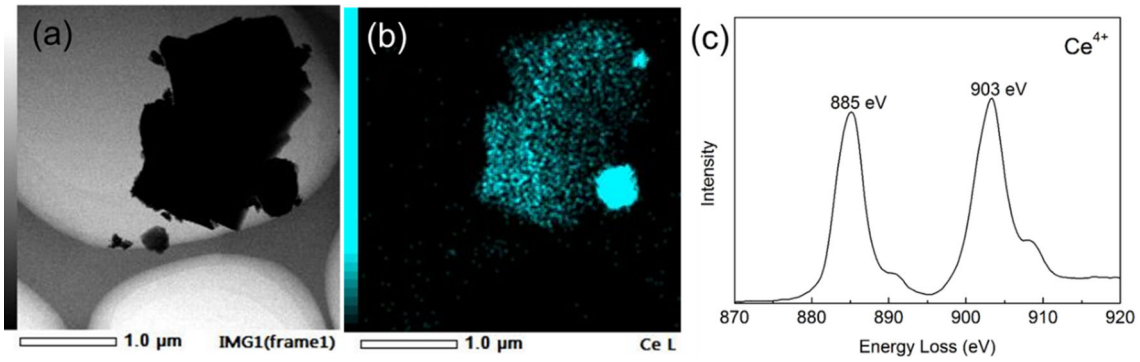

Figure 2. TEM analysis of Ce-containing glass: (**a**) TEM image of glass particles, (**b**) EDS elemental mapping to show Ce element distribution in glass and (**c**) EELS of Ce element.

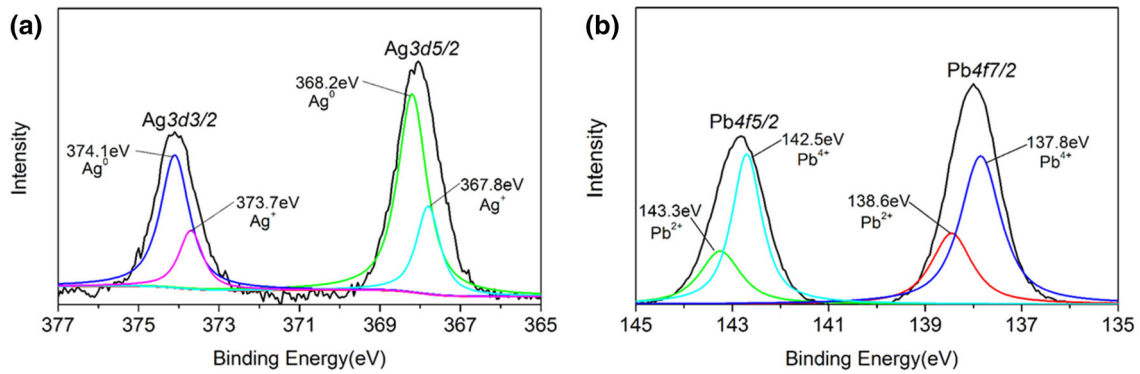

Figure 3. XPS spectra of (**a**) Ag and (**b**) lead elements in the glass.

Figure 4a and b presents the SEM images of glasses prepared with and without addition of Ag powder, respectively. It can be clearly observed in figure 4b that in the Ag-containing glass numerous nano-sized Ag particles were embedded. The presence of Ag colloids in the glasses can also be evidenced by the UV–visible absorption spectrum (figure 4c), in which plasma resonance absorption peaks were exhibited. It was observed that with increasing Ag content in glass preparation, the plasma resonance absorption strength of glasses was also enhanced, implying the increase in the number of Ag colloids formed in glasses [14,15].

3.2 *Effect of Ag colloids in glass on resistivity of Ag/Si contact*

A special Ag/glass/Si interface structure was formed during the sintering of Ag paste on the Si wafers with a pyramid-textured surface structure, which was prepared by a chemical etching method in terms of solar cell application. By using the TLM method, the resistivity of the Ag/Si contact was measured, as shown in figure 5. The results indicated clearly that the application of glasses containing Ag colloids can substantially reduce the resistivity of the Ag/Si contact. In the case of Ag-free glass, the resistivity of the Ag/Si

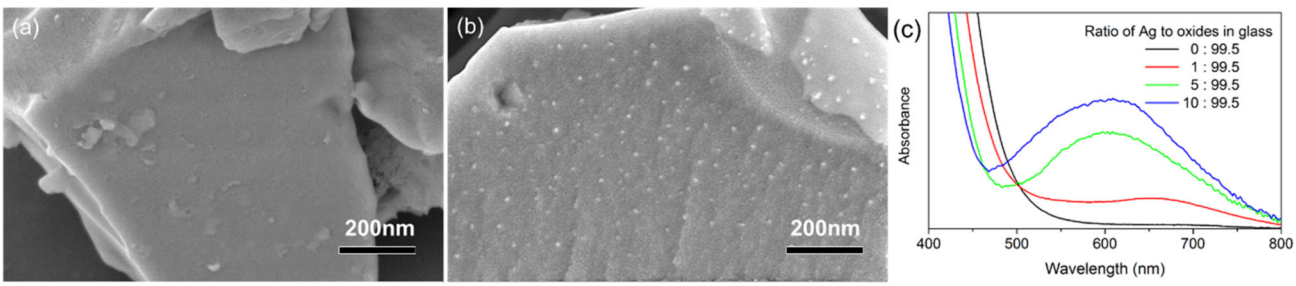

Figure 4. SEM images of glass powder (**a**) containing Ag and (**b**) not containing Ag. (**c**) UV–visible spectra of glasses containing different contents of Ag.

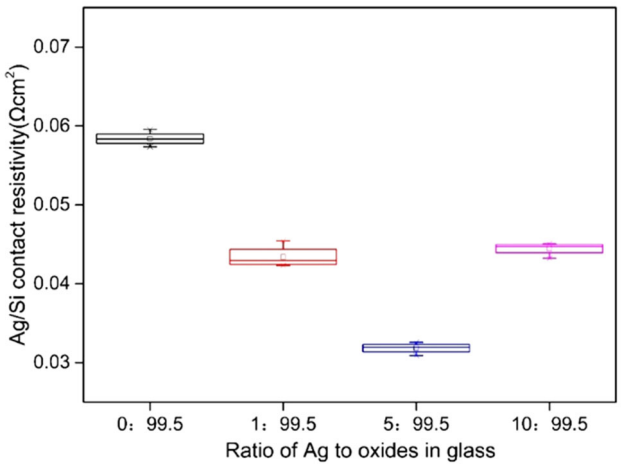

Figure 5. Resistivity of the Ag/Si contact with different ratios of Ag to oxides in glass.

contact was about 0.058 Ω cm^2; whereas it decreased to 0.043 and 0.032 Ω cm^2 as the ratio of Ag to oxides in glass was 1:99.5 and 5:99.5, respectively, which declined as much as 25.86 and 62.07%. However, when the ratio of Ag to oxides further increased to 10:99.5, the resistivity of the Ag/Si contact decreased to 0.045 Ω cm^2. This implies that the excessive dissolution of Ag in the glass phase at the interface may cause some damage to the Ag/Si contact based on the following equation [5]:

$$Ag^{+} + Si \rightarrow Ag^{0} + Si^{4+} \quad (4)$$

The sintered Si surface in contact with Ag paste was studied by SEM. Figure 6a–d displays the images of Si surface covered with the glass phase, where the upper layer of the sintered Ag paste has been removed using nitric acid. It can be clearly observed that when Ag-free glass was used, very few Ag colloids were there on the Si surface resulting from the reaction during the sintering of Ag paste (figure 6a). In contrast, the amount of Ag colloids formed on the Si surface of Ag-containing glasses becomes significantly greater, and it increased obviously by an increase in the Ag content (figure 6b–d). After removing the glass layer using hydrofluoric acid, the bare Si surface becomes visible, as shown in figure 6e–h. It can be clearly observed that the pyramid-textured structure of Si surface was corroded by the glass phase in different degrees depending on the Ag content in glasses. Ag-free glass had slight erosion on the Si surface (figure 6e). With the increase of Ag content in glasses, the erosion of Si surface became more and more serious. For example, figure 6f shows that the pyramid tips on the Si wafer were eroded by the glass in which the ratio of Ag to oxides was 1:99.5. Such damage became more obvious when the ratio increased to 5:99.5, which led to some small eroded holes (figure 6g). When the ratio further increased to 10:99.5, very serious erosion was caused. The top of the pyramids was almost completely flattened and a large number of deep pits were formed (figure 6h).

As far as the Ag/Si contact formed by the metallization of Ag paste is concerned, if the erosion of glass on the Si surface is serious, it is not conducive to reduction of the resistivity of the contact [16]. For example, figure 6h shows that the glass caused much damage and defect to the Si surface, which must cause large leakage and recombination during carrier transport across the Ag/Si contact. Moreover, the surface of the Si wafers was doped heavily with phosphorus, whose concentration was distributed as an erfc function profile (figure 7a). Therefore, a slight erosion may result in great decrease of carrier concentration on the Si surface. According to the resistance formula of ohmic contact between a metal and semiconductor based on the tunnelling mechanism:

$$R_c \propto \exp(\phi_s/\sqrt{N_D}) \quad (5)$$

where ϕ_s is the barrier height of the semiconductor side and N_D is the dopant concentration; the contact resistance increases with the decrease of dopant concentration on the Si surface. It was proposed that the Ag colloids in the interface glass phase can reduce the ϕ_s. By using the ECV

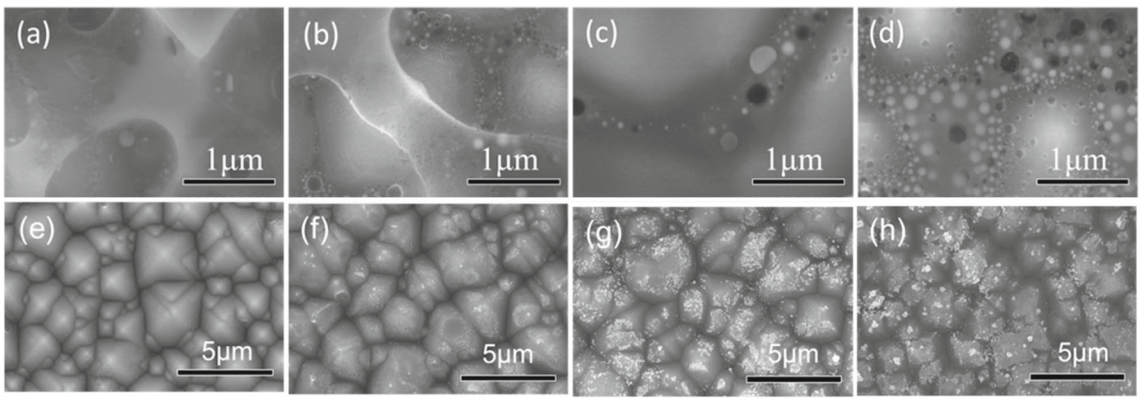

Figure 6. SEM images of sintered Ag/Si contact interface. (**a–d**) The surface where the Ag electrodes were removed and the interface glass layer was exposed. (**e–h**) The surface where both the Ag electrodes and glass layer were removed. Here the ratios of Ag to oxides in glass are (**a**, **e**) 0:99.5, (**b**, **f**) 1:99.5, (**c**, **g**) 5:99.5 and (**d**, **h**) 10:99.5, respectively.

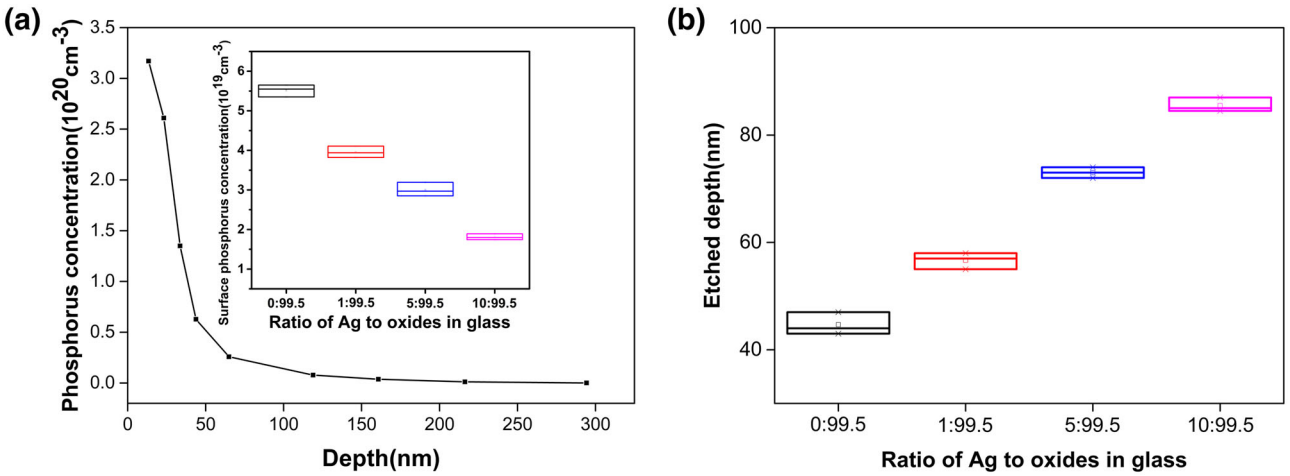

Figure 7. (**a**) Phosphorus concentration distribution curve of a raw Si wafer before Ag paste metallization on it. The inset in (**a**) shows the surface phosphorus concentrations of Si wafers after Ag paste metallization using glass with different ratios of Ag to oxides. (**b**) Etched depths of Si wafers by Ag paste metallization, which were estimated according to the surface phosphorus concentrations.

method, the dopant concentration of the Si surface in contact with glasses containing different contents of Ag was measured. The surface dopant concentration of raw Si wafers was 3.2×10^{20} cm^{-3} (figure 7a). After co-sintering of Ag paste, in which the ratios of Ag to oxides in glass were 0:99.5, 1:99.5, 5:99.5 and 10:99.5, the dopant concentrations of Si surfaces decreased to 5.5×10^{19}, 4.0×10^{19}, 2.9×10^{19} and 1.8×10^{19} cm^{-3} (inset in figure 7a), respectively. The corresponding etched depths of Si surface were estimated to be 47, 56, 73 and 87 nm (figure 7b), respectively. For this reason, the resistivity of the Ag/Si contact increased significantly as the ratio of Ag to oxides in glass increased from 5:99.5 to 10:99.5 (figure 5).

The use of Ag-containing glass in Ag paste can really improve the quality of metallization ohmic contact on Si wafers, and thus greatly promote the electrical performance of c-Si solar cells. In the current study, two cells are compared, of which one employed Ag-free glass (no. 5) and another employed Ag-containing glass (no. 7, in which the ratio of Ag to oxides in glass was 5:99.5). According to the *I–V* cell characterization results presented in table 2, the cell efficiency with the Ag-containing glass showed a 0.95 percentage increase compared to what was achieved with the Ag-free glass. This notable advancement is attributed to the substantial decrease in the cell series resistance (R_s) by about 3.1 mΩ due to the decrease of resistivity of the Ag/Si contact (figure 5). Such a decrease in R_s resulted in great increase in the fill factor (FF) by nearly 3.48 percentage. Comparatively, the open circuit voltage (V_{oc}) and short circuit current (I_{sc}) of the two cells were close.

Table 2. *I–V* cell characterization results.

Glass code	η (%)	V_{oc} (mV)	I_{sc} (A)	FF (%)	R_s (mΩ)
No. 5	20.83	676.1	9.895	76.76	5.4
No. 7	21.78	676.6	9.896	80.24	2.3

The measured values (0.032–0.058 Ω cm^2) of resistivity of the Ag/Si contact in our case are less than that (0.1 Ω cm^2) suggested by Cabrera *et al* [17] to form a glass layer on top of the Si substrate. Ren *et al* [18] also achieved a resistivity of Ag/Si contact of 0.31–0.84 Ω cm^2, and attributed the lower values to the formation of Ag_2Te and PbTe crystallites in the reformed tellurite glass underlying the front Ag gridline. With PbO–TeO_2–SiO_2–Bi_2O_3–Li_2O–RO (R = Na, Zn or B) glass, Kim *et al* [19] found that the resistivity of the contact decreased from 0.033 to 0.001 Ω cm^2 as the fraction of area of Ag crystallites on the Si surface increased from 1.8 to 13.2%. Kontermann *et al* [20] even tested a much smaller value of 0.047 mΩ cm^2 on the contact between an Ag crystallite and Si substrate. Although the resistivity of the contact between Ag or Ag_2Te crystallites and Si substrate is low, the recombination at the contact is much high to degrade the V_{oc} of solar cells. For example, the V_{oc} reported in [18,19] was no more than 640 mV. In contrast, the Ag/Si contact through a thin layer of Ag-colloid containing glass has low recombination, and outputs high V_{oc}, e.g., 676 mV as presented in table 2. As a consequence, the efficiency of our solar cells can reach more than 21%.

4. Conclusion

In the current study, we demonstrated a strategy for producing large amounts of Ag colloids in the PbO–TeO_2–SiO_2 glass system by precipitating the $Ce_{1.88}Pb_{2.12}O_{6.53}$ crystal to increase the solubility of Ag in glasses. By applying these Ag colloid-containing glasses in the Ag paste metallization on Si wafers, it has been definitely confirmed that the resistivity of the Ag/Si contact decreased substantially. However, it was also found that too high content of Ag

dissolved in glasses may destroy the pyramid-textured surface structure of Si wafers, which is disadvantageous to Ag/Si ohmic contact due to the formation of surface defects and the decrease of dopant concentration on the Si surface. Therefore, to obtain the minimum resistivity of the Ag/Si contact, it is necessary to balance the number of Ag colloids formed with the erosion of Ag on the Si surface.

Acknowledgement

This study was supported by the Shanghai Science and Technology Committee Project (Number 17DZ1201102).

References

[1] Schubert G, Beaucarne G, Tous L and Hoornstra J 2019 *AIP Conference Proceedings* p 020002
[2] Li Z, Liang L and Cheng L 2009 *J. Appl. Phys.* **105** 066102
[3] Kumar P, Aabdin Z, Pfeffer M and Eibl O 2018 *Sol. Energy Mater. Sol. Cells* **178** 52
[4] Hong K K, Cho S B, You J S, Jeong J W, Bea S M and Huh J Y 2009 *Sol. Energy Mater. Sol. Cells* **93** 898
[5] Fields J D, Ahmad M I, Pool V L, Yu J, Van Campen D G, Parilla P A *et al* 2016 *Nat. Commun.* **7** 11143
[6] Hong K K, Cho S B, Huh J Y, Park H J and Jeong J W 2009 *Met. Mater. Int.* **15** 307
[7] Kumar P, Pfeffer M, Willsch B and Eibl O 2016 *Sol. Energy Mater. Sol. Cells* **145** 358
[8] Pysch D, Mette A, Filipovic A and Glunz S W 2009 *Prog. Photovoltaics: Res. Appl.* **17** 101
[9] Cho S B, Hong K K, Huh J Y, Park H J and Jeong J W 2010 *Curr. Appl. Phys.* **10** S222
[10] Cheng S, Yang G, Zhao Y, Peng M, Skibsted J and Yue Y 2015 *Sci. Rep.* **5** 17526
[11] Gayathri Pavani P, Sadhana K and Chandra Mouli V 2011 *Physica B* **406** 1242
[12] Cui S, Le Coq D, Boussard-Plédel C and Bureau B 2015 *J. Alloys Compd.* **639** 173
[13] Pavlo Z and Philippe G S 2010 *ACS Nano* **10** 5599
[14] Satoshi T, Kiyoshi Y and Kiyoshi M 2010 *J. Non-Cryst. Solids* **265** 133
[15] Simo A, Polte J, Pfander N, Vainio U, Emmerling F and Rademann K 2012 *J. Am. Chem. Soc.* **134** 18824
[16] Vinod P N 2007 *J. Mater. Sci.: Mater. Electron.* **19** 594
[17] Cabrera E, Olibet S, Glatz-Reichenbach J, Kopecek R, Reinke D and Schubert G 2011 *Energy Procedia* **8** 540
[18] Ren K, Unsur V, Chowdhury A, Zhang Y and Ebong A 2018 *WCPEC-7 & IEEE PVSC* **46** p 1051
[19] Kim Y, Huh J and Kim H 2018 *Sol. Energy Mater. Sol. Cells* **185** 97
[20] Kontermann S, Willeke G and Bauer J 2010 *J. Appl. Phys. Lett.* **97** 191910